

# Amphiphilic Thermoresponsive Poly(Hydroxyaminoethers) as Effective Emulsifiers for Preparation of Waterborne Epoxy Resins

Ying-Chi Huang, Li-Ting Wang, Shu-Wei Hsu, Tai-Fu Lin, Ying-Chih Liao, Wen-Ying Chiu, Hsin-Wei Lin, Chien-Hsin Wu,\* Ru-Jong Jeng,\* and Shih-Huang Tung\*

Amphiphilic poly(hydroxyaminoethers) (PHAEs) with thermoresponsive solubility in aqueous solutions are developed in this study. Through the control of stoichiometric ratios of functional groups and the reaction temperature, a series of PHAEs with different hydrophilic segments is synthesized, as evidenced by proton nuclear magnetic resonance ( $^1\text{H-NMR}$ ) and Fourier transform infrared (FT-IR) spectroscopy. These PHAEs could be dissolved in aqueous solutions and exhibit the thermal phase transitions with lower critical solution temperatures (LCSTs) due to the hydrogen bonding between the hydrophilic segments and water, as confirmed by differential scanning calorimetry (DSC). In addition, the hydrophilic-lipophilic balance (HLB) values suggest that the PHAEs are more hydrophilic amphiphiles and suitable for use as oil-in-water emulsifiers. Consequently, commercially available epoxy resins can be successfully stabilized by the PHAEs in water to form stable emulsions. These crosslinkable waterborne epoxy resins show good thermal and resistance properties, and the feasibility in anticorrosion coating applications for steel surfaces is demonstrated.

difunctional nucleophiles, exhibiting notable thermal, mechanical, and substrate-adhesion properties. PHAEs also show an impressive barrier quality in packing applications. Intermolecular hydrogen bonding interactions cause low oxygen and carbon dioxide transmission rates that are comparable to those of poly(ethylene terephthalate) (PET) widely used in soft drink bottles.<sup>[1]</sup> Furthermore, the partial miscibility of PHAEs with several polymers could be attributed to specific intermolecular interactions, such as hydrogen bonding interactions between the lateral hydroxyl groups of PHAEs and the ester group of PET.<sup>[2,3]</sup> A biodegradability can be realized by blending PHAEs with biodegradable polymers, such as poly(caprolactone)<sup>[4]</sup> or poly(butylene adipate-co-terephthalate).<sup>[5,6]</sup> PHAEs also exhibit several biomaterial-related advantages, such as hydrolytic stability

of chemical structures and good hydrophilicity, due to their hydroxyl groups.<sup>[7]</sup> The PHAEs with cationic nature can inhibit inflammatory cell recruitment and are potential to be used as the coatings for biomedical devices.<sup>[7]</sup> New properties and novel functionalities are still under exploration as numerous monomers can be potential candidates for synthesizing PHAEs.

Synthetic amphiphilic polymers dispersible in aqueous media have been widely used in industrial applications; for example, they can serve as waterborne polymers themselves or can be employed as emulsifiers and dispersants to stabilize hydrophobic polymers in water for both environmental and economic purposes.<sup>[8–15]</sup> Demand is still increasing for waterborne polymers that can reduce the usage of organic solvents and meet stricter regulations for the release of volatile organic compounds. Usually, noncovalent interactions, such as van der Waals forces, hydrogen bonds, or ionic interactions, determine the overall solubility of amphiphilic polymers in water. Highly polar groups, including ether linkages, hydroxyl groups, or amino groups, can be introduced to improve the affinity between polymers and water molecules. Depending on the number, position, or sequence of polar sites, amphiphilic polymers show various conformation and intermolecular interactions with water in aqueous solutions.

Amphiphilic polymers in aqueous solutions may exhibit unique structures along with thermoresponsive conformations.

## 1. Introduction

Poly(hydroxyaminoethers) (PHAEs) are a class of epoxy-based thermoplastic polymers composed of bisepoxides and various

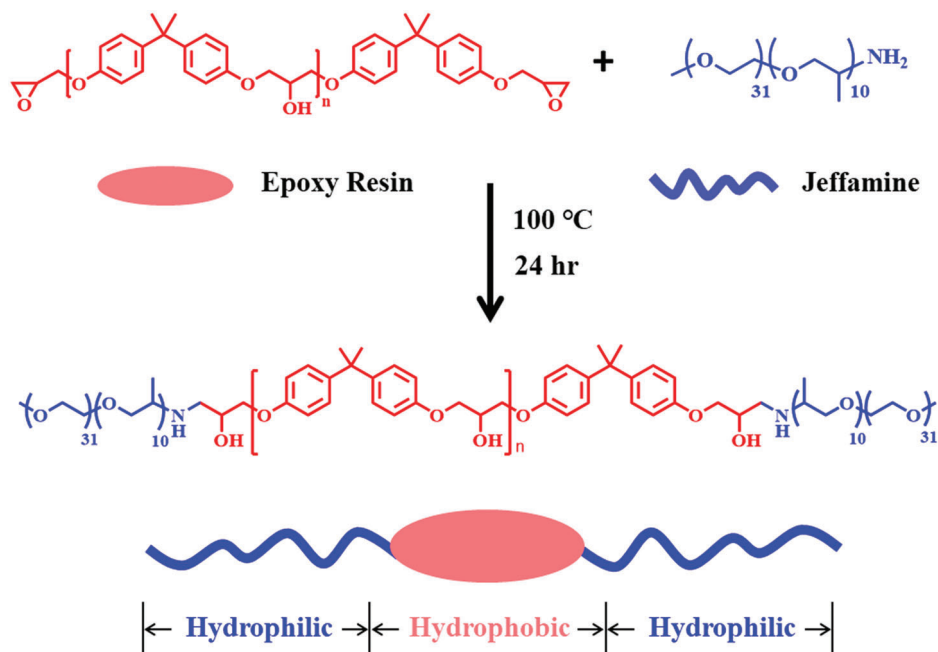
Y.-C. Huang, L.-T. Wang, S.-W. Hsu, T.-F. Lin, C.-H. Wu, R.-J. Jeng, S.-H. Tung  
 Institute of Polymer Science and Engineering  
 and Advanced Research Center for Green Materials Science and Technology  
 National Taiwan University  
 Taipei 10617, Taiwan  
 E-mail: chwuoliver@ntu.edu.tw; rujong@ntu.edu.tw;  
 shtung@ntu.edu.tw

Y.-C. Liao, W.-Y. Chiu  
 Department of Chemical Engineering  
 National Taiwan University  
 Taipei 10617, Taiwan

H.-W. Lin  
 China Steel Corporation  
 Kaohsiung 81233, Taiwan

 The ORCID identification number(s) for the author(s) of this article can be found under <https://doi.org/10.1002/mame.202100668>

DOI: 10.1002/mame.202100668



**Scheme 1.** Synthesis scheme of amphiphilic PHAEs.

For those with well-defined hydrophilic and hydrophobic segments, such as amphiphilic block copolymers, various self-assembled structures, including spheres, cylinders, worm-like micelles, or vesicles, are observed in water, mainly driven by the hydrophobic interaction.<sup>[16,17]</sup> For some hydrophilic chains, such as those with oxyethylene units,<sup>[18–21]</sup> when the temperature increases, a coil-globule transition occurs because the chain conformation is dominated by the competition between the monomer-water and monomer-monomer hydrogen bonding in the aqueous solution. The collapse of polymer chains leads to aggregation and phase separation at the lower critical solution temperature (LCST). As a result, the thermoresponsive emulsion particle size or solubility can be realized.<sup>[9,22–24]</sup>

In our previous study, we have developed the comb-like PHAEs under mild conditions in the absence of solvents or catalysts and the PHAEs can self-disperse in an aqueous solution.<sup>[25]</sup> However, due to a high fraction of the soft hydrophilic etheramines that are required for self-dispersion, the comb-like PHAEs show relatively low glass transition temperatures (< 50 °C), which may limit the applications of the PHAEs, especially for those in need of high thermal and mechanical properties. In the present study, a series of robust amphiphilic PHAEs with reversible water solubility were newly developed for the preparation of epoxy oil-in-water emulsions. The synthetic procedures involved applying a selective amine-epoxide reaction between primary and secondary amine functional groups, which were confirmed using <sup>1</sup>H-NMR and Fourier transform infrared (FT-IR) spectroscopy. The aqueous suspension structures and the amphiphilicity of the PHAEs were investigated using small-angle x-ray scattering (SAXS) techniques and hydrophilic-lipophilic balance (HLB) values, respectively. The PHAEs that contain hydrophilic oxyethylene chains show phase behaviors with LCSTs along with reversible solubility in aqueous solutions. By using the amphiphilic PHAEs as emulsifiers, we could directly accomplish the oil-in-

water microencapsulation of epoxy resin without additional surfactants or ionization processes. The waterborne epoxy resins emulsified by the PHAEs developed in this work are potential for the applications in crosslinkable coatings with high mechanical and resistance properties.

## 2. Experimental Section

### 2.1. Materials

The epoxy resins based on diglycidyl ether of bisphenol A (DGEBA), including E1000 ( $M_n \approx 1000$ , catalog number: BE501), E1250 ( $M_n \approx 1250$ , BE502), E1520 ( $M_n \approx 1520$ , BE503), E1630 ( $M_n \approx 1630$ , BE504), and E6000 ( $M_n \approx 6000$ , BE509) were provided by Chang Chun Plastics Co., Ltd., Taiwan. The DGEBA-based epoxy resin E340 (340 g mol<sup>-1</sup>) was purchased from Sigma-Aldrich. The polyether amine, methoxy poly(oxyethylene-oxypropylene)-2-propylamine (Jeffamine M2070,  $M_n \approx 2000$  g mol<sup>-1</sup>), was provided by Huntsman Corp. The solvents used in this work, including acetone and methyl ethyl ketone (MEK), were distilled under reduced pressure over MgSO<sub>4</sub> or CaH<sub>2</sub> and stored over 4-Å molecular sieves.

### 2.2. Synthesis of Amphiphilic PHAEs

Taking the synthesis of the PHAE from the DGEBA-based epoxy resin E1000 ( $M_n \approx 1000$  g mol<sup>-1</sup>) as an example, in a typical polymerization procedure (**Scheme 1**), the epoxy resin (6.25 g, 6.25 mmol) was dissolved in Jeffamine M2070 (25.0 g, 12.5 mmol) at 100 °C in a 500-mL, four-necked flask equipped with a mechanical stirrer, reflux condenser, thermometer, and nitrogen inlet. The reaction was maintained at 100 °C for 24 h, allowing the ring-opening reaction of epoxides with amine groups.

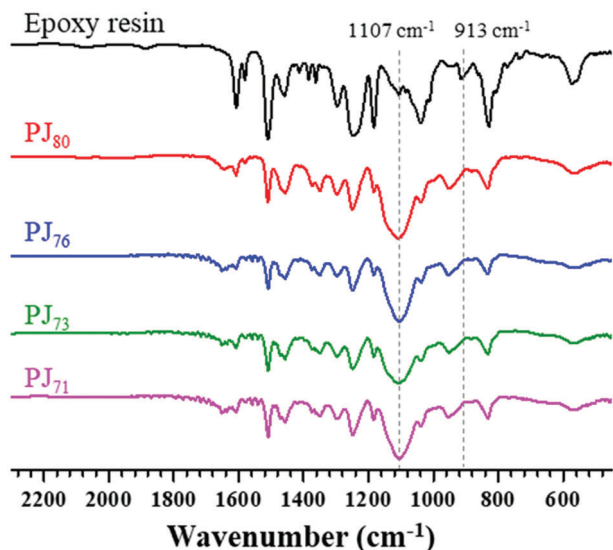


**Figure 1.** FT-IR spectra of PHAEs.

The product was named PJ<sub>80</sub> where the subscript number was the weight fraction of the hydrophilic etheramine segment. The products of the three other epoxy resins with E1250, E1520, and E1630 treated with Jeffamine M2070 were PJ<sub>76</sub>, PJ<sub>73</sub>, and PJ<sub>71</sub>, respectively.

The successful syntheses of the desired PHAEs were confirmed through FT-IR (Figure 1) and <sup>1</sup>H-NMR (Figure 2) spectroscopy. FT-IR (KBr) spectroscopy data were as follows: 1509 and 1608 cm<sup>-1</sup> (p-sub, benzene ring quadrant stretching), 1107 cm<sup>-1</sup> (C–N stretching vibrations), absence of 913 cm<sup>-1</sup> (ring vibration of epoxy ring), and 831 cm<sup>-1</sup> (1,4-substitution of aromatic ring). <sup>1</sup>H NMR (400 MHz, d-CDCl<sub>3</sub>, δ) spectroscopy returned the following values: 1.10 (d, J = 5.00 Hz, 14.28H), 1.56 (s, 6.04H), 2.66 (m, 0.98H), 2.80 (s, 0.50H), 3.36 (s, 4.67H), 3.45 (m, 9.10), 3.59 (s, 61.69H), 3.88 (m, 1.52H), 4.03 (s, 3.19H), 4.26 (s, 0.77H), 6.75 (d, J = 6.80 Hz, 4.00H), and 7.04 (d, J = 7.00 Hz, 4.04H).

### 2.3. Emulsification of Waterborne Epoxy Resins Using PHAEs

The synthesized PHAEs were used to emulsify the DGEBA-based epoxy resins in water through the phase inversion method, one resin with high molecular weight ( $M_n \approx 6000 \text{ g mol}^{-1}$ , E6000) and one with low molecular weight ( $M_n \approx 340 \text{ g mol}^{-1}$ , E340). The epoxy resins, E6000 or E340, and the PHAEs were first dissolved in MEK at room temperature under 2000-rpm stirring for 1 h (Scheme 2), where the weight ratio of epoxy resin:PHAE:MEK was 20:3:17. Subsequently, deionized water was added to the epoxy resin solution by using a syringe pump at a rate of 1 g min<sup>-1</sup> and the final water/oil weight ratio was 0.5. Reduced pressure distillation was applied at room temperature to remove MEK, producing white emulsions of PJ<sub>80</sub>(E340), PJ<sub>80</sub>(E6000), PJ<sub>76</sub>(E6000), PJ<sub>73</sub>(E6000), and PJ<sub>71</sub>(E6000) with approximately 50% solid content.

### 2.4. Instrumentations

The functional groups of the PHAEs were examined using a Jasco 4100 FT-IR spectrophotometer with a Jasco ATR Pro 450-S accessory. <sup>1</sup>H-NMR spectra were obtained using a Bruker Avance-400 MHz FT-NMR spectrometer with chloroform-d or dimethyl sulfoxide-d<sub>6</sub> as the solvents. The gel permeation chromatogram (GPC) was performed on a series of GPC KD-802, KD-804, and KD-806 separation columns using DMF as the eluent. Glass transition temperature ( $T_g$ ) and melting temperature ( $T_m$ ) were measured using a differential scanning calorimeter (DSC, TA Instruments, Discovery 25) under an N<sub>2</sub> atmosphere. Thermogravimetric analysis (TGA) was performed on a Q50 thermogravimetric analyzer (TA instruments) operating at a heating rate of 10 °C min<sup>-1</sup> under N<sub>2</sub> atmosphere.

SAXS experiments for the determination of the PHAE micelle size in water (1 wt.%) were carried out on the BL23A1 beamline in the National Synchrotron Radiation Research Center (NSRRC), Taiwan. The scattering curves were obtained with a monochromatic beam of wavelength  $\lambda = 0.83 \text{ \AA}$  at room temperature. The data were shown as plots of the absolute intensity  $I(q)$  versus wave vector  $q = 4\pi\sin\theta/\lambda$ , where  $\theta$  is the scattering angle.<sup>[26,27]</sup> For the measurement of LCSTs, PHAEs were dissolved in deionized water at a concentration of 5 mg/100 mL and the samples were investigated by DSC at a heating rate of 1 °C min<sup>-1</sup>. For amphiphilicity measurement, the oils for emulsification were first prepared by mixing turpentine (HLB = 16) and cottonseed oil (HLB = 6) at varying weight ratios, resulting in linearly averaged HLB values ranging from 6 to 16. 5wt% of the PHAEs and 15wt% of the oils were then mixed, followed by the addition of 80wt% deionized water. The mixtures were treated with ultrasonication for 15 min. The stability levels of the emulsions were then subjected to naked eye examination after 12 h to determine the HLB values of the PHAEs.

The particle size distributions of the emulsions (0.1 mg mL<sup>-1</sup>) were determined by the dynamic light scattering (DLS) technique (90 Plus, Brookhaven Instrument Corp.) with a 15-mW solid-state laser ( $\lambda = 675 \text{ nm}$ ). The zeta potentials of the particles were determined by the same instrument. Scanning electron microscopy (SEM) images were taken by a JEOL JSM-6330F microscope. 0.1 wt.% of the emulsions were freeze-dried and then sputtered with platinum prior to imaging. The sedimentation behaviors of the emulsions were analyzed using a dispersion analyzer (LUMiSizer, LUM). 2-mm rectangular cuvettes were filled with 0.4 mL of the 50-wt% solid content of emulsion. The cuvettes were capped and centrifuged at 2000 ( $\approx 500 \text{ g}$ ), 2500 ( $\approx 790 \text{ g}$ ), 3000 ( $\approx 1100 \text{ g}$ ), and 3500 rpm ( $\approx 1500 \text{ g}$ ) for up to 5000 s at 25 °C. Every 10 s, light transmission profiles were captured at  $\lambda = 865 \text{ nm}$  throughout the cell to quantify the sedimentation velocity of particles.<sup>[28–30]</sup> The sedimentation velocity under normal gravity was estimated by extrapolation of the measured sedimentation velocity at high relative centrifugation forces (RCF) to 1 g. Corrosion tests were performed by coating polymer emulsion on steel plates (70 × 150 mm<sup>2</sup>) followed by treatment with ASTM B117 standard in a salt spray cabinet.<sup>[31,32]</sup>

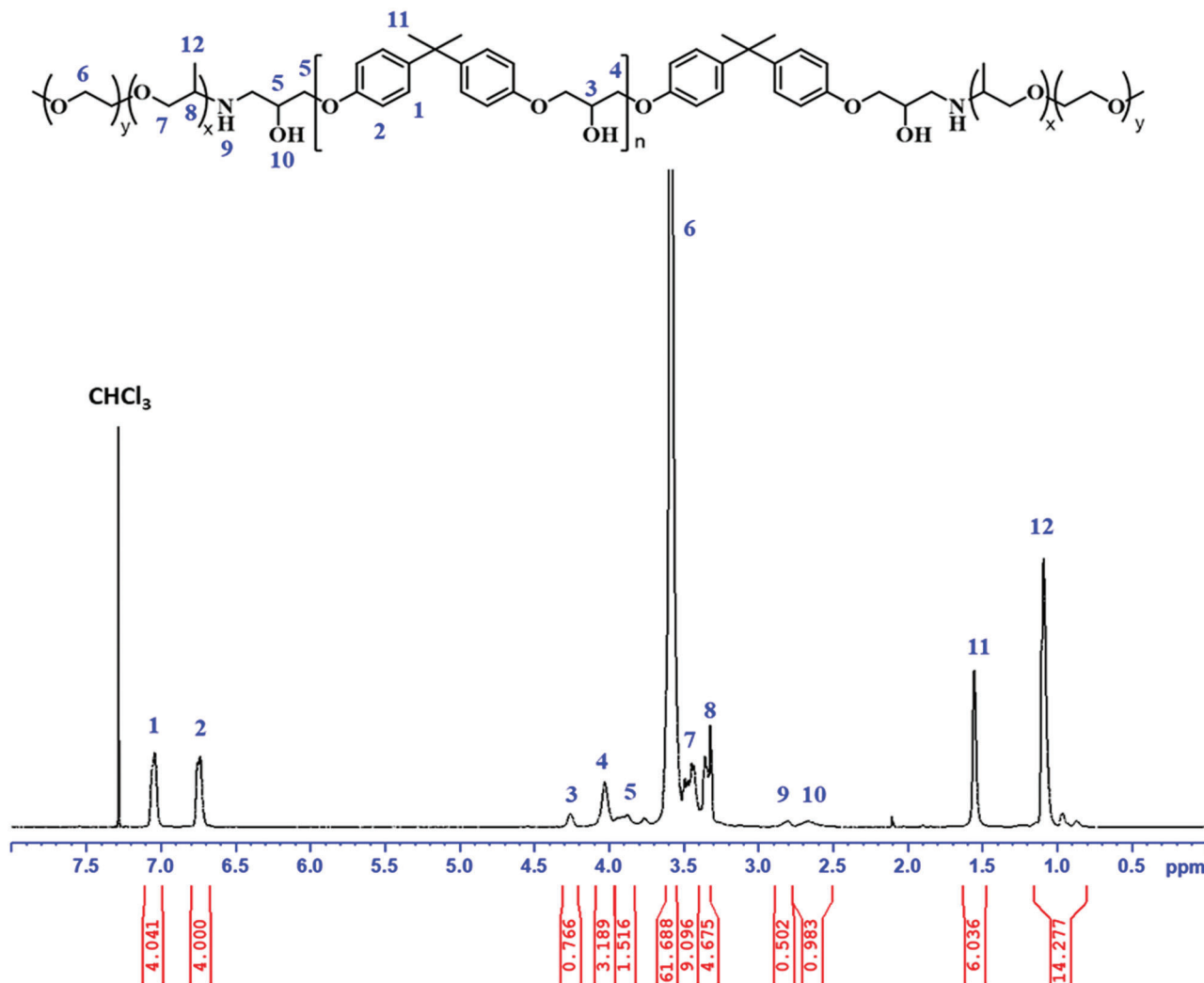


Figure 2.  $^1\text{H-NMR}$  spectra of PJ80.

## 2.5. SAXS Modeling

The particle size and distribution were obtained by model fitting for the SAXS data.<sup>[26,27,33]</sup> The scattering intensity  $I(q)$  can be modeled by the form factor  $P(q)$  of the scatterers in the dilute system where the interaction between scatterers was neglected. The SAXS scattering spectra of the PHAEs aqueous solutions were fitted using the Schulz sphere model. The model function is given by:

$$I(q) = N_0(\Delta\rho)^2 \left(\frac{4}{3}\Pi\right)^2 \int_0^\infty f(R)R^6 F^2(qR) dR \quad (1)$$

where  $\Delta\rho$  is the difference in scattering length density between the scatter and the solvent.  $R$  is the particle radius.  $N_0$  is the total number of particles per unit volume. The scattering amplitude of a single particle was determined as follows:

$$F(qR) = \frac{3[\sin(qR) - qR \cos(qR)]}{(qR)^3} \quad (2)$$

The Schulz distribution equation  $f(R)$  was used to describe the polydispersity of the particle radius as follows:

$$f(R) = \left(\frac{z+1}{R_0}\right)^{z+1} \frac{R^z}{\Gamma(z+1)} \exp\left[-(z+1)\frac{R}{R_0}\right] \quad (3)$$

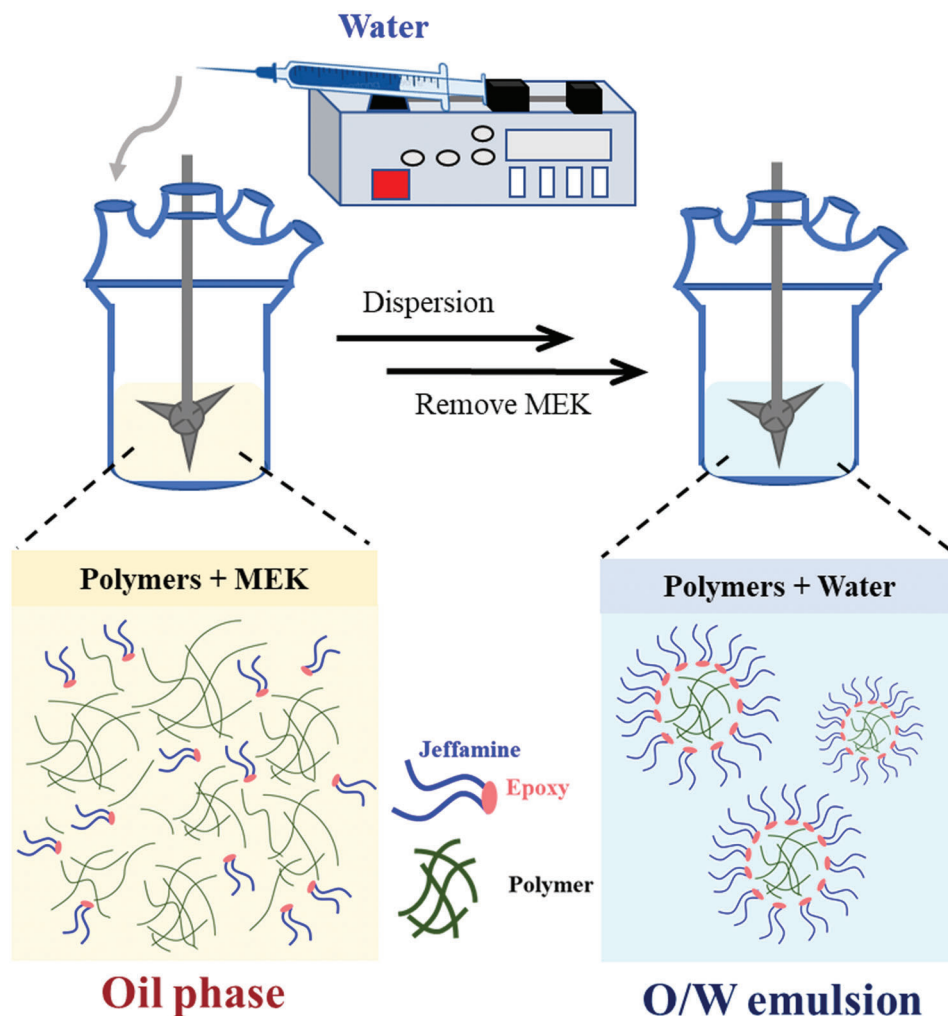
where  $R_0$  is the average particle radius,  $\Gamma$  is the gamma function, and  $z$  is a parameter related to the width of the distribution. The polydispersity index  $p$  is defined by

$$p = \frac{1}{\sqrt{z+1}} \quad (4)$$

## 3. Results and Discussion

### 3.1. Characterization of PHAEs

Amphiphilic PHAEs were prepared through the reactions between the epoxide groups and the primary amine groups



**Scheme 2.** Preparation of oil-in-water emulsions by the phase inversion method.

**Table 1.** Formulation, molecular weights, thermal properties, and micellization of the PHAEs.

Sample	Composition		Formulation and molecular weight			Thermal properties		Micellization	
	Epoxy[P]	Jeffamine[J]	$M_n^a$ [g mol <sup>-1</sup> ]	$M_w/M_n^b$	J % <sup>c</sup> [wt.%]	$T_{ds}^d$ [°C]	$T_g^e$ [°C]	$R_0^f$ [nm]	$p^g$
PJ <sub>80</sub>	E1000	M2070	7625	1.24	80	292	-51	3.9 ± 0.009	0.29
PJ <sub>76</sub>	E1250	M2070	8175	1.31	76	295	-54	4.7 ± 0.006	0.25
PJ <sub>73</sub>	E1520	M2070	8741	1.37	73	310	-51	5.2 ± 0.005	0.27
PJ <sub>71</sub>	E1630	M2070	8562	1.33	71	301	-49	5.5 ± 0.005	0.27

<sup>a)</sup> Determined by calibration of epoxy molecular weight using GPC; <sup>b)</sup> determined by GPC; <sup>c)</sup> weight percentage of Jeffamine M2070 in the polymer; <sup>d)</sup> 5% weight loss temperature determined by TGA; <sup>e)</sup> glass transition temperature determined by DSC; <sup>f)</sup> average radius determined by SAXS; <sup>g)</sup> polydispersity index determined by SAXS.

(Scheme 1). By taking advantage of the faster reaction rate of primary amine-epoxide over secondary amine-epoxy, the reactions could be carried out at lower temperatures (< 100 °C) to prevent the secondary amine-epoxy reaction.<sup>[34]</sup> The covalently-bonded Jeffamine M2070 in the PHAEs, along with the formation of secondary amine bearing the hydroxyl group ( $\beta$ -amino alcohols) after the ring-opening of oxirane, acted as hydrophilic segments that provided polar sites for

enhancing polymer solubility in water. The bisphenol-A-based epoxy chains in the PHAEs were the hydrophobic segments. The products synthesized from E1000, E1250, E1520, and E1630 epoxies treated with Jeffamine M2070 were named PJ<sub>80</sub>, PJ<sub>76</sub>, PJ<sub>73</sub>, and PJ<sub>71</sub>, respectively, where the subscript numbers are the weight fractions of the hydrophilic etheramine segments. The formulations of all the PHAEs are summarized in **Table 1**.



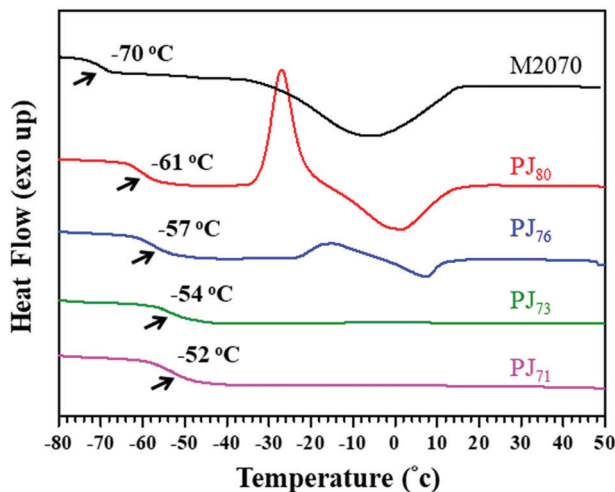


Figure 3. DSC thermograms of PHAEs.

The polymerization processes were monitored by FT-IR as shown in Figure 1. For neat epoxy resins, the adsorption peak at  $913\text{ cm}^{-1}$  was attributed to the  $\text{-C-O-C-}$  stretching vibration of epoxide groups.<sup>[35]</sup> After polymerization, the disappearance of the epoxide absorption peak at  $913\text{ cm}^{-1}$  along with a newly emerged absorption peak of the C-N group at  $1107\text{ cm}^{-1}$  indicated the completion of the PHAE product reactions. Due to the incorporation of the bisphenol-A-based epoxy resins, the absorption peaks for the C-C stretching vibrations in the aromatic ring were recorded at  $1509$  and  $1608\text{ cm}^{-1}$  and the peaks at  $1038$  and  $1249\text{ cm}^{-1}$  were attributed to the symmetrical and asymmetrical stretching of the aromatic ether group, as depicted in Figure 1. The successful synthesis of the representative  $\text{PJ}_{80}$  was verified through  $^1\text{H-NMR}$  (Figure 2) by comparing the chemical shifts with those of the neat bisphenol-A-based epoxy resin (Figure S3, Supporting Information). The disappearance of the signals at  $\delta = 2.66, 2.80,$  and  $3.36\text{ ppm}$  for the oxirane group and the appearance of the peak at  $3.88\text{ ppm}$  confirmed the formation of  $\text{PJ}_{80}$ . The molecular weights of the PHAEs were evaluated using GPC (Figure S1, Supporting Information). As listed in Table 1, the number average molecular weights ( $M_n$ ) of the PHAEs from GPC were comparable to the theoretical molecular weights based on the stoichiometric ratios.<sup>[36]</sup> The PDIs of the PHAEs were in the range between 1.24–1.33. The TGA data in Figure S4, Supporting Information, and Table 1 show that the 5-wt% weight loss temperature ( $T_{d5}$ ) of the PHAEs are over  $290\text{ }^\circ\text{C}$  and increases with decreasing fraction of the hydrophilic segments.

Thermal phase transitions such as glass transition ( $T_g$ ), crystallization temperature ( $T_c$ ), and melting temperature ( $T_m$ ) were measured through DSC analysis as shown in Figure 3 and summarized in Table 1. In the second heating at a rate of  $10\text{ }^\circ\text{C min}^{-1}$ , neat M2070 exhibited a  $T_g$  of  $-70\text{ }^\circ\text{C}$  and a  $T_m$  of  $-5\text{ }^\circ\text{C}$ . The  $T_g$ s of the neat epoxy resins for the synthesis of the PHAEs increased with increasing molecular weight and ranged from  $37$  to  $60\text{ }^\circ\text{C}$ . As the content of epoxy resins increased, the rigid aromatic moieties restricted the molecular motion of the PHAEs and thus the  $T_g$ s of the PHAEs increased, from  $\text{PJ}_{80}$  of  $-61\text{ }^\circ\text{C}$  to  $\text{PJ}_{71}$  of  $-52\text{ }^\circ\text{C}$ . The increased epoxy resin content also limited the regular packing of the polyether diamine segments. Consequently, the

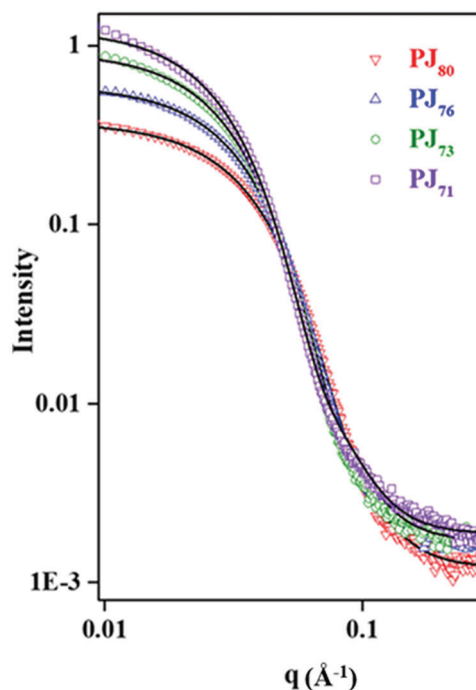


Figure 4. SAXS data of the amphiphilic PHAEs dissolved in water at 1 wt.% concentration.

enthalpy of melting for the  $\text{PJ}_{80}$  and  $\text{PJ}_{76}$  samples decreased and  $\text{PJ}_{73}$  and  $\text{PJ}_{71}$  recorded negligible melting signals during the second heating run, indicating a lower crystallinity of the polyether diamine segments in the PHAEs.

### 3.2. Micellization of PHAEs in Water

The PHAEs were found to be highly soluble in aqueous solutions and formed micelles due to their amphiphilicity. The SAXS profiles of the dilute PHAEs aqueous solution at 1wt% concentration are shown in Figure 4 where the model fittings (Equations (1)–(4) in Section 2.5) are presented as the solid curves through the data. The fitting parameters are listed in Table 1. The radii of the micelles ranged from  $3.9\text{ nm}$  for  $\text{PJ}_{80}$  to  $5.5\text{ nm}$  for  $\text{PJ}_{71}$ , increasing with decreasing fraction of the hydrophilic segments.

Interestingly, the PHAE aqueous solutions exhibited pronounced phase transition in response to temperature upon heating and cooling as shown in Figure 5a. When the temperature increased from room temperature to  $85\text{ }^\circ\text{C}$ , the transparent solutions became opaque, indicating a large-scale aggregation of the polymers at  $85\text{ }^\circ\text{C}$ . In other words, the solution exhibited an LCST behavior. The precipitated polymer underwent a coil-globule transition due to the weakening of hydrogen bonding between polyether segments and water molecules, leading to the interchain aggregation and phase separation at the LCST.<sup>[37,38]</sup> When the PHAE solutions were cooled to room temperature, the polyether segments reformed the hydrogen bonding with water and thus extended the coils to increase water solubility. Consequently, the PHAEs were restored to small micelles and the solutions turned back to be transparent, manifesting a thermally-reversible behavior.

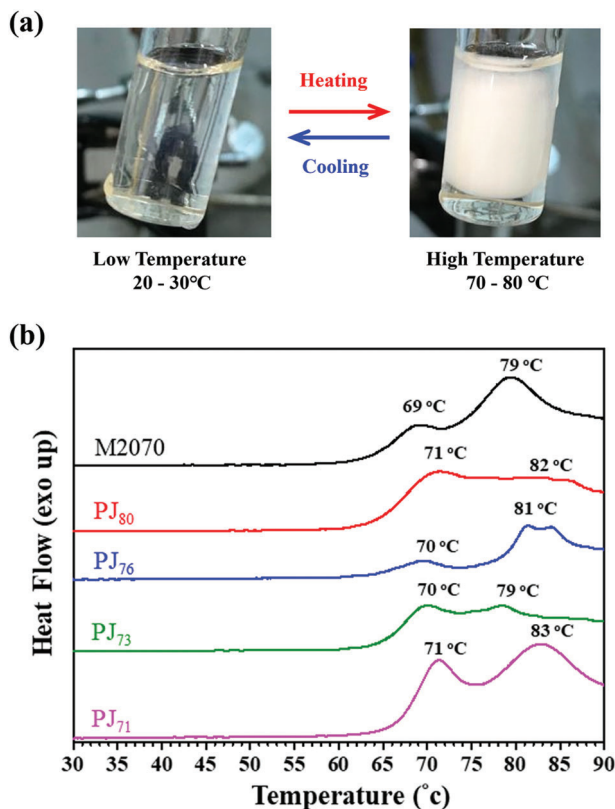


**Figure 5.** a) Photographs of reversible phase transition for PJ<sub>80</sub> in water upon heating and cooling and b) DSC thermograms of the M2070 and the PHAE aqueous solutions.

The LCST phase behaviors of the neat M2070 and the PHAE aqueous solutions at 5 wt.% concentration were investigated using DSC at a heating rate of 1 °C min<sup>-1</sup>, as shown in Figure 5b. Multiple exothermic peaks were found between 60 and 85 °C for the neat M2070 as well as the PHAEs, confirming the occurrence of the phase transitions caused by the polyether segments at elevated temperatures. The exothermic behavior implied that the transitions were originated from the enthalpy effect, that is, the formation of the intra- and inter-polyether interactions at the expense of the intermolecular ones between the polyethers and water molecules lowered the total enthalpy at LCST. The multiple peaks on the DSC thermograms may be attributed to the relatively complicated chemical structure that originated from the

copolymerization of the ethylene oxide and propylene oxide units in polyethers.<sup>[39]</sup>

The amphiphilicity of the PHAEs was evaluated using the HLB values. A set of mixed oils composed of cottonseed oil (HLB = 6) and turpentine (HLB = 16) at different mass ratios were prepared and the HLB values of the mixed oils were linearly calculated ranging from 6 to 16.<sup>[40–42]</sup> The HLB value of the oil that could be best emulsified by the PHAE in water was taken as the HLB value of the PHAE. As shown in Figure S5, Supporting Information, the HLB values of PJ<sub>80</sub>, PJ<sub>76</sub>, and PJ<sub>73</sub> were determined to be 14 and that of PJ<sub>71</sub> was 13, consistent with the lower fraction of the hydrophilic segments in PJ<sub>71</sub>. The PHAEs with HLB values above 13 are more hydrophilic amphiphiles that form clear solutions when dissolved in water, and are good candidates for the use as oil-in-water emulsifiers.<sup>[43]</sup> The emulsification of epoxy resins using these PHAEs is discussed in the following section.

### 3.3. Emulsification and Applications

The use of the PHAEs to emulsify hydrophobic epoxy resins in water by the phase inversion method is illustrated in Scheme 2. Neat high- and low-M<sub>n</sub> epoxy resins, E6000 or E340, and the PHAEs were dissolved in MEK first and then the deionized water was added, followed by reduced pressure distillation to remove MEK. The PHAEs could successfully work as emulsifiers to stabilize E6000 and E340 in water. The particle sizes of the PJ<sub>80</sub>(E6000), PJ<sub>76</sub>(E6000), PJ<sub>73</sub>(E6000), and PJ<sub>71</sub>(E6000) emulsions determined by DLS are listed in Table 2. The particle sizes increased with decreasing fraction of hydrophilic segments on the PHAEs and the average sizes based on volume distribution ranged from 649 to 963 nm. The SEM images of freezing-dried particles from the emulsions are shown in Figure 6. The particles are nearly spherical and the size ranged from 500 to 1000 nm, consistent with the DLS results. The zeta potentials ( $\zeta$ ) of the particles were around 40 mV due to the protonation of the amine groups, which also led to weak basic emulsions with pH values between 8 and 9.

The emulsion stability was evaluated by the particle sedimentation velocity measured using a dispersion analyzer. The sedimentation velocities of the particles were estimated from the light transmission profiles as functions of time and position over the entire samples under various centrifugal forces.<sup>[26–28]</sup> The sedimentation velocities were then plotted against the RCF as shown in Figure S6, Supporting Information, and the velocity under normal gravity was determined by extrapolation to a gravity of

**Table 2.** Thermal properties of E6000-based oil-in-water emulsions.

Sample	Emulsion					$T_{d5}^c$ [°C]	$T_g^d$ [°C]
	Size (Volume) <sup>a</sup> [nm]	PDI <sup>a</sup>	$\zeta^b$	pH	Sedimentation velocity [mm/day]		
PJ <sub>80</sub> (E6000)	649 ± 37	0.01	41	8.5	0.05	361	62
PJ <sub>76</sub> (E6000)	825 ± 92	0.01	39	8.2	0.08	362	64
PJ <sub>73</sub> (E6000)	860 ± 122	0.01	44	8.7	0.03	362	66
PJ <sub>71</sub> (E6000)	963 ± 109	0.05	44	8.4	0.12	363	68

<sup>a</sup> Particle sizes and PDI determined by DLS; <sup>b</sup> zeta potential; <sup>c</sup> 5% weight loss temperature determined by TGA; <sup>d</sup> glass transition temperature determined by DSC.

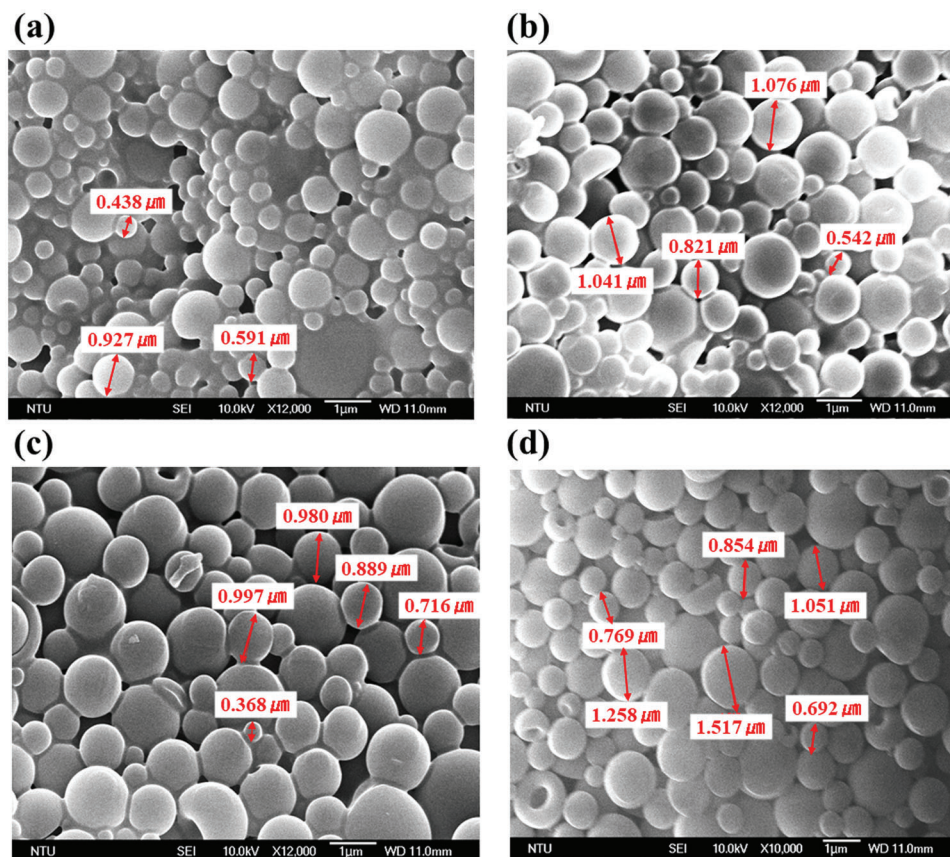


**Figure 6.** SEM images of emulsions after freeze drying: a)  $PJ_{80}(E6000)$ , b)  $PJ_{76}(E6000)$ , c)  $PJ_{73}(E6000)$ , and d)  $PJ_{71}(E6000)$ .

1 g. As shown in Table 2, the sedimentation velocities of the emulsions range from 0.03 to 0.12 mm/day, that is, an overall movement distance less than 7.2 mm after 2 months. These results imply that the epoxy resins emulsified by the amphiphilic PHAEs are rather stable at room temperature. Furthermore, the amphiphilic PHAEs show thermoresponsive emulsification due to their LCST behaviors as described in the preceding section. Taking  $PJ_{80}(E340)$  emulsion as an example, when the temperature was increased from 25 to 85 °C, the well-dispersed emulsion separated into two distinct phases, as shown in Figure 7. When the temperature was cooled to room temperature, the emulsion recovered. The result demonstrates a thermally-reversible emulsification by means of the LCST behavior of the emulsifiers in aqueous solutions.

The dried samples cast from the  $PJ(E6000)$  emulsions show  $T_{ds}$ s over 360 °C and  $T_g$ s between 62–68 °C, as listed in Figure S7, Supporting Information, and Table 2. With such a good thermal stability and a low content of volatile organic compounds, these crosslinkable waterborne epoxy resins are potential for applications in an environmentally-friendly manner. The application of the PHAE emulsions as the coatings on the steel surface to act as the protective layer was demonstrated. As displayed in Figure 8, when the steel was coated with the  $PJ_{80}(E340)$  whose  $T_g$  is –22 °C, distinct rust areas that were yellow-brown in color were observed under a spray of 5-wt% salt solution in a cabinet according to the ASTM B117 standard. In contrast, as the steel was coated with

$PJ_{80}(E6000)$ , the corrosion test results were greatly improved and the steel showed a nearly defect-free surface. The emulsion of  $PJ_{80}(E6000)$  has a much higher  $T_g$  (62 °C) compared with that of  $PJ_{80}(E340)$  and thus can provide more rigid and robust protection at room temperature. Similar dependence of the coating performance on  $T_g$  has been noted in the previous study.<sup>[25]</sup> This result demonstrated the possibility of creating waterborne epoxy resin emulsions by using PHAEs for the anticorrosion coating.



#### 4. Conclusion

A series of amphiphilic PHAEs with various hydrophilic segment contents that exhibit thermoresponsive solubility in aqueous solutions was accomplished. The PHAEs were synthesized through the selective amine–epoxide reaction between primary and secondary amine functional groups, as verified using <sup>1</sup>H-NMR and FT-IR spectra. Due to the hydrophilic polyether segments that provide hydrogen bonding sites for water molecules, the PHAEs can dissolve in water and form spherical micelles with sizes less than 5.5 nm, as determined by SAXS technique. The hydrogen bonding sites between polymer and water molecules were broken at temperatures above 85 °C as indicated in the DSC analysis, leading to the unique thermal phase transitions at LCST. With an HLB value above 13, the PHAEs can work as emulsifiers to stabilize epoxy resins in water and form oil-in-water emulsions. The

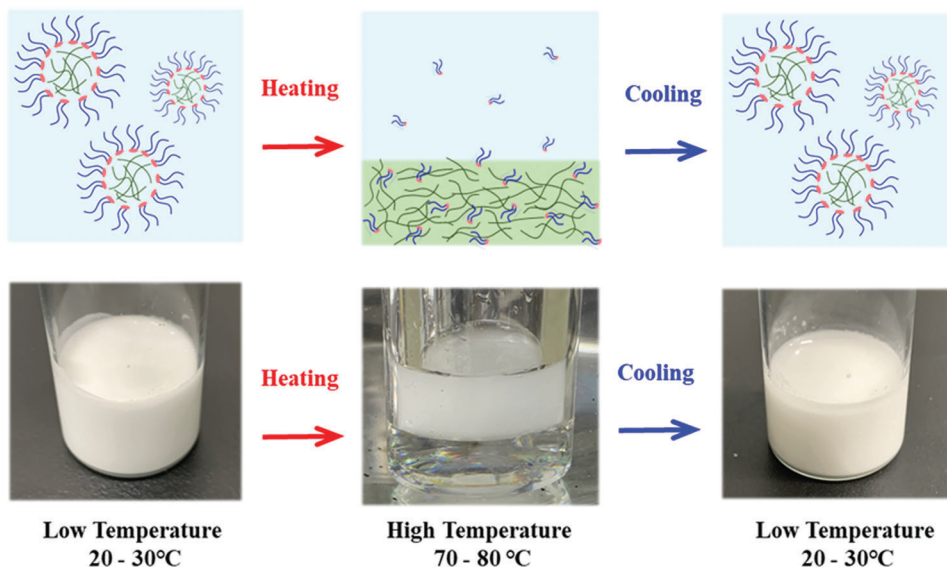




**Figure 7.** Reversible phase transition for PJ<sub>80</sub>(E340) dispersed in water.

Sample	PJ <sub>80</sub> (E340)	PJ <sub>80</sub> (E6000)
Photo		
T <sub>g</sub> (°C)	-22	62

**Figure 8.** Photographs of steel surfaces coated with PJ<sub>80</sub>(E340) and PJ<sub>80</sub>(E6000) after salt spray corrosion test for 24 h following ASTM B117 standard.

crosslinkable waterborne epoxy resins demonstrate their feasibility for use in anticorrosion coating applications on steel surfaces.

## Supporting Information

Supporting Information is available from the Wiley Online Library or from the author.

## Acknowledgements

This work was financially supported by the Ministry of Science and Technology in Taiwan (MOST 109-2622-8-006-005, 110-2634-F-002 -043, and 109-2622-E-002-029). This article was subsidized for English editing by National Taiwan University under the NTU Excellence Improvement Program for Doctoral Students (108-2926-I-002-002-MY4), sponsored by the Ministry of Science and Technology, Taiwan.

## Conflict of Interest

The authors declare no conflict of interest.

## Data Availability Statement

The data that support the findings of this study are available in the supplementary material of this article.

## Keywords

corrosion resistance, poly(hydroxyaminoethers), reversible solubility, waterborne epoxy resins

Received: September 7, 2021  
Revised: November 5, 2021  
Published online: December 23, 2021

- [1] J. E. White, H. C. Silvis, M. S. Winkler, T. W. Glass, D. E. Kirkpatrick, *Adv. Mater.* **2000**, *12*, 1791.
- [2] A. Granado, J. I. Eguiazabal, J. Nazabal, *Macromol. Mater. Eng.* **2006**, *291*, 1074.

- [3] A. Granado, J. I. Eguiazábal, J. Nazábal, *Macromol. Mater. Eng.* **2004**, 289, 997.
- [4] M. Á. Corres, Á. Mayor, A. Sangroniz, J. del Río, M. Iriarte, A. Etxeberria, *Eur. Polym. J.* **2020**, 135, 109869.
- [5] A. Sangroniz, L. Sangroniz, N. Aranburu, M. Fernández, A. Santamaria, M. Iriarte, A. Etxeberria, *Eur. Polym. J.* **2018**, 105, 348.
- [6] A. Sangroniz, L. Sangroniz, A. Gonzalez, A. Santamaria, J. del Rio, M. Iriarte, A. Etxeberria, *Eur. Polym. J.* **2019**, 115, 76.
- [7] M. Ma, W. F. Liu, P. S. Hill, K. M. Bratlie, D. J. Siegwart, J. Chin, M. Park, J. Guerreiro, D. G. Anderson, *Adv. Mater.* **2011**, 23, H189.
- [8] H. Homma, S. Kubo, T. Yamada, Y. Matsushita, Y. Uraki, *J. Wood Chem. Technol.* **2008**, 28, 270.
- [9] M. C. Tatry, P. Galanopoulo, L. Waldmann, V. Lapeyre, P. Garrigue, V. Schmitt, V. Ravaine, *J. Colloid Interface Sci.* **2021**, 589, 96.
- [10] A. Kumar, S. Li, C. M. Cheng, D. Lee, *Ind. Eng. Chem. Res.* **2015**, 54, 8375.
- [11] J. Zhang, M. R. Dubay, C. J. Houtman, S. J. Severtson, *Macromolecules* **2009**, 42, 5080.
- [12] S.-W. Kuo, *Polym. Int.* **2021**, <https://doi.org/10.1002/pi.6264>.
- [13] M. G. Mohamed, E. C. Atayde, B. M. Matsagar, J. Na, Y. Yamauchi, K. C. W. Wu, S.-W. Kuo, *J. Taiwan Inst. Chem. Eng.* **2020**, 112, 180.
- [14] W.-C. Su, F.-C. Tsai, C.-F. Huang, L. Dai, S.-W. Kuo, *Polymers* **2019**, 11, 201.
- [15] Y.-T. Shieh, P.-Y. Lin, S.-W. Kuo, *Polymer* **2018**, 143, 258.
- [16] A. Blanazs, S. P. Armes, A. J. Ryan, *Macromol. Rapid Commun.* **2009**, 30, 267.
- [17] E. B. Zhulina, O. V. Borisov, *Macromolecules* **2012**, 45, 4429.
- [18] M. Shibata, T. Terashima, T. Koga, *Macromolecules* **2021**, 54, 5241.
- [19] S. Sugihara, S. Kanaoka, S. Aoshima, *Macromolecules* **2005**, 38, 1919.
- [20] S. Sun, P. Wu, *Macromolecules* **2013**, 46, 236.
- [21] T. Isono, K. Miyachi, Y. Satoh, S.-i. Sato, T. Kakuchi, T. Satoh, *Polym. Chem.* **2017**, 8, 5698.
- [22] B. H. L. Oh, A. Bismarck, M. B. Chan-Park, *Biomacromolecules* **2014**, 15, 1777.
- [23] M. Arotçaréna, B. Heise, S. Ishaya, A. Laschewsky, *J. Am. Chem. Soc.* **2002**, 124, 3787.
- [24] J. V. M. Weaver, I. Bannister, K. L. Robinson, X. Bories-Azeau, S. P. Armes, M. Smallridge, P. McKenna, *Macromolecules* **2004**, 37, 2395.
- [25] C.-H. Wu, Y.-C. Huang, T.-H. Lai, S.-H. Chiu, N. Uchibe, H.-W. Lin, W.-Y. Chiu, S.-H. Tung, R.-J. Jeng, *Polymer* **2020**, 196, 122464.
- [26] S. Kuchler, T. Detloff, T. Sobisch, D. Lerche, *Ceram. Forum Int.* **2011**, 88, E27.
- [27] D. Lerche, *J. Dispersion Sci. Technol.* **2002**, 23, 699.
- [28] H. N. Yow, S. Biggs, *Soft Matter* **2013**, 9, 10031.
- [29] T. J. Prosa, B. J. Bauer, E. J. Amis, *Macromolecules* **2001**, 34, 4897.
- [30] H.-M. Chang, C.-Y. Lin, S.-H. Tung, *Soft Matter* **2020**, 16, 3505.
- [31] S. M. Cambier, G. S. Frankel, *Electrochim. Acta* **2014**, 136, 442.
- [32] G. Matamala, W. Smeltzer, G. Droguett, *Corros. Sci.* **2000**, 42, 1351.
- [33] M. Nayeri, M. Zackrisson, J. Bergenholtz, *J. Phys. Chem. B* **2009**, 113, 8296.
- [34] J.-E. Ehlers, N. G. Rondan, L. K. Huynh, H. Pham, M. Marks, T. N. Truong, *Macromolecules* **2007**, 40, 4370.
- [35] H. Abdollahi, A. Salimi, M. Barikani, A. Samadi, S. Hosseini Rad, A. R. Zanjanijam, *J. Appl. Polym. Sci.* **2019**, 136, 47121.
- [36] T. P. Skourlis, R. L. McCullough, *J. Appl. Polym. Sci.* **1996**, 62, 481.
- [37] Q. Zhang, C. Weber, U. S. Schubert, R. Hoogenboom, *Mater. Horiz.* **2017**, 4, 109.
- [38] W. S. Cai, L. H. Gan, K. C. Tam, *Colloid Polym. Sci.* **2001**, 279, 793.
- [39] J. L. G. Ribelles, M. S. Sanchez, L. T. de la Osa, I. Krakovský, *J. Non-Cryst. Solids* **2005**, 351, 1254.
- [40] W. Zhang, K. Wang, X. Hu, X. Zhang, S. Chang, H. Zhang, *Polym. Adv. Technol.* **2020**, 31, 2127.
- [41] X. Meng, H. Liu, Y. Xia, X. Hu, *Carbohydr. Polym.* **2021**, 258, 117653.
- [42] Y.-L. Lin, M.-Z. Wu, Y.-J. Sheng, H.-K. Tsao, *J. Chem. Phys.* **2012**, 136, 104905.
- [43] H. T. Davis, *Colloids Surf., A* **1994**, 91, 9.